Breakup of an Active Chiral Fluid

Luke Neville,[1,2,3,*] Jens Eggers,[2,†] and Tanniemola B. Liverpool[2,3,‡]
[1]Department of Physics, Massachusetts Institute of Technology, Cambridge, Massachusetts 02139, USA
[2]School of Mathematics, Fry Building, University of Bristol, BS8 1UG, Bristol, United Kingdom
[3]The Isaac Newton Institute for Mathematical Sciences, Cambridge CB3 0EH, United Kingdom

(Received 16 July 2025; accepted 21 April 2026; published 19 August 2026; corrected 21 October 2026)

We study the breakup dynamics of a two-dimensional strip of active chiral fluid using continuum hydrodynamics. Using slender body theory, we show that the breakup is driven by the interplay between chiral and surface tension forces, and that the minimum strip thickness decays to zero as a power law in finite time. The power law exponent and corresponding scaling function describing the shape of the strip near the break point are computed analytically, and shown to be in excellent agreement with numerical simulations of the underlying hydrodynamics. Qualitative agreement between experiment and simulation is also found.

DOI: 10.1103/w2n2-zzkd

The decay of a fluid stream into drops is a highly nonlinear process, driven in passive systems by surface tension forces pulling in the stream from its surface [1–4]. Little is known, however, when the fluid is active, or composed of individual agents that use energy to do work on their environment. These fluids, which show a variety of collective phenomena not seen in normal liquids [5,6], differ from their passive counterpart by driving themselves unstable from the inside out [6–9]. The effect of activity on interface dynamics has typically been studied in the linear or near-linear regimes. For example, small deviations from a flat interface [10] or in active phase separation [8,11] determining the long-time scaling and size-distribution of stable droplets. Here, we look at the highly nonlinear dynamics near breakup of an unstable active film.

In particular, we examine a new type of fluid breakup where the instability is driven by the persistent spin of each constituent particle [12–17], which on hydrodynamic scales manifests itself as an antisymmetric contribution to the stress tensor. Because the spin only affects the stress, these active chiral fluids behave identically to ordinary fluids in their bulk, with all effects of chirality propagating inward from the boundaries [18]. These effects were demonstrated in recent experiments [12] on a two-dimensional chiral fluid, made by sedimenting millions of particles onto a table and spinning them up with rotating magnetic fields [19]. Taking thin strips of this chiral fluid, the authors of [12] observed counter-propagating flows along the strip boundaries, which eventually led to breakup as the boundaries came into contact and sheared the fluid apart (see Fig. 1). This linear instability was then compared against the predictions

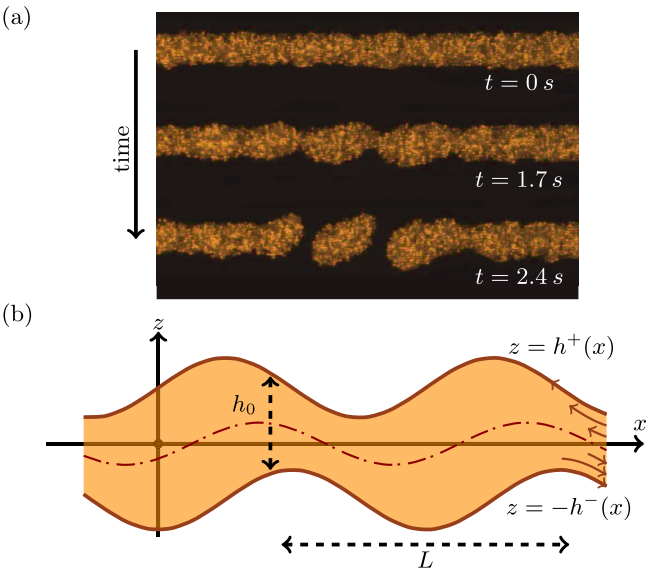


FIG. 1. (a) Experimental evidence of two dimensional strips of chiral fluid breaking up asymmetrically, provided courtesy of the William Irvine group. The arrow marks the direction of time, with the strip going unstable before breaking up into drops. The whole process happens in a few seconds. (b) Sketch of a strip of chiral fluid undergoing an instability leading to breakup. The top and bottom surfaces are at $z = \pm h^{\pm}(x)$, the characteristic vertical scale is h_0, the horizontal scale is L, and their ratio is $\epsilon = h_0/L$. The dot-dashed orange line marks the centerline of the strip at $z = c(x)$, and the arrows inside the strip show the chiral shear flows.

*Contact author: lajn@mit.edu
†Contact author: jens.eggers@bristol.ac.uk
‡Contact author: t.liverpool@bristol.ac.uk

Published by the American Physical Society under the terms of the Creative Commons Attribution 4.0 International license. Further distribution of this work must maintain attribution to the author(s) and the published article's title, journal citation, and DOI.

from a hydrodynamic theory of chiral fluids, with excellent agreement found. The purpose of this Letter is to go beyond the linear regime and study the fully nonlinear dynamics involved in breakup.

Our analysis uses asymptotics based upon slenderness to derive equations for the strip evolution. With these, we show that the strip evolves self-similarly near breakup, with the minimum thickness decreasing to zero as a power law in finite time. The corresponding scaling exponent is anomalous [20,21] and cannot be derived from dimensional considerations; it instead comes from solving a nonlinear eigenvalue problem that arises from a scaling analysis [4]. These predictions perfectly match results from full simulations of the partial differential equations (PDE), and qualitatively agree with experimental data.

Hydrodynamics—Consider the strip of chiral fluid shown in Fig. 1. In the fluid bulk, interparticle forces are balanced against the friction each particle feels from the glass substrate. Using $\boldsymbol{\sigma}$ for the stress tensor and $\boldsymbol{u}$ for the velocity, this gives

$$\boldsymbol{\nabla}\cdot\boldsymbol{\sigma}-\Gamma\boldsymbol{u}=\boldsymbol{0}, \tag{1}$$

where Γ is the friction coefficient of the substrate [12,22,23]. For chiral systems, it is known [12,24,25], that these hydrodynamic stresses can be described by a modified Newtonian stress tensor

$$\sigma_{ij}=\eta(\nabla_i u_j+\nabla_j u_i)-p\delta_{ij}+\eta_R\epsilon_{ij}(2\Omega-\omega), \tag{2}$$

where η is the dynamic viscosity, p is the pressure enforcing incompressibility, and η_R is the rotational viscosity [16]. The rotational viscosity term captures the friction felt whenever the spin rate of the particles, Ω, is different to that of the surrounding water $\omega/2=\epsilon_{ij}\nabla_i u_j/2$ [24,25]. In a passive system, conservation of angular momentum ensures the equality of the these spin rates and so the rotational viscosity term vanishes; for the chiral systems considered here, Ω is constant and set by the external driving [12]. Substituting the stress tensor (2) into (1) we find

$$(\eta+\eta_R)\nabla^2\boldsymbol{u}-\boldsymbol{\nabla}p-\Gamma\boldsymbol{u}=\boldsymbol{0}, \tag{3}$$

showing that chirality acts only to shift the viscosity in the fluid bulk. These chiral fluids therefore act the same as an ordinary fluids when surrounded by solid walls, as the no-slip boundary condition does not involve the particle spin, Ω.

This spin, however, is picked up at free surfaces, where the boundary condition, coming from a balance of stress and surface tension, is

$$\boldsymbol{\sigma}\cdot\boldsymbol{n}=-\gamma(\boldsymbol{\nabla}\cdot\boldsymbol{n})\boldsymbol{n}, \tag{4}$$

where $\boldsymbol{n}$ is the unit outward normal to the chiral fluid, γ is the coefficient of surface tension [26,27], and $\boldsymbol{\nabla}\cdot\boldsymbol{n}$ is the mean curvature of the interface. The experimentally measured values of all parameters can be found in Soni *et al.* [12].

Using (x,z) for coordinates in the down and cross strip direction, respectively, the top and bottom free surfaces have position $z=\pm h^{\pm}(x)$ [see Fig. 1(b)], and evolve in time according to the kinematic boundary condition

$$h_t^{\pm}+uh_x^{\pm}=\pm v|_{z=\pm h^{\pm}}, \tag{5}$$

where $(u,v)=\boldsymbol{u}$, and subscripts denote derivatives. For a passive fluid we would expect the strip to evolve symmetrically with $h^+=h^-$, but chiral stresses break this symmetry. For later use we note that the height functions are related to the strip center-line and half-thickness by $c=(h^+-h^-)/2$ and $h=(h^++h^-)/2$, respectively.

One-dimensional reduction—To understand chiral breakup we must tackle the nonlinear dynamics of $h^{\pm}$ contained in Eqs. (1), (4), and (5), which can be difficult even with a sophisticated numerical method. We will take an alternative approach, exploiting the slenderness of the strip to project the dynamics down into one dimension [2,4,28–31].

One-dimensional reductions have proven extremely successful in other problems [28,29,32], and follow the ideas of slender-body theory, expanding the dynamics in a small parameter given by the ratio of the strips thickness to its horizontal length scale. Leaving the derivation to Supplemental Material [33], we find

$$\begin{aligned}\Gamma c_t&=-\frac{4\eta\eta_R\Omega}{\eta+\eta_R}\frac{h_x}{h}+\gamma\frac{c_{xx}}{h},\\ \Gamma h_t&=-\frac{4\eta\eta_R\Omega}{\eta+\eta_R}(hc_x)_{xx}+\gamma(c_xc_{xx}-hh_{xxx})_x,\end{aligned} \tag{6}$$

which are two equations for the strip center line and thickness. Keeping the parameters makes clear the origin of each term: those proportional to Ω come from the chiral stress, while others proportional to γ come from surface tension. A linear stability analysis of Eq. (6) reproduces, at small initial thickness, the behavior of the full equations [12].

To go beyond the linear regime, we must integrate (6) numerically to understand nonlinearities. Our simulations were performed with periodic boundary conditions, using a well-tested finite difference method [4,28,34]. Spatial derivatives were approximated to second order on a highly refined grid, which was adapted to scale with the pinch region. Time integration was done using the fully implicit step-halving method, ensuring both stability and second-order accuracy [33,35].

An example of a nonlinear evolution is shown in Fig. 2(a), where the initial shape is drawn in light orange, and a sequence of darkening lines shows the strip as time progresses. The final shape, which we shade in orange, pinches off at the origin. Despite the profiles looking antisymmetric, the thickness function h is symmetric about the pinchpoint, with all asymmetry in the strip coming from the totally

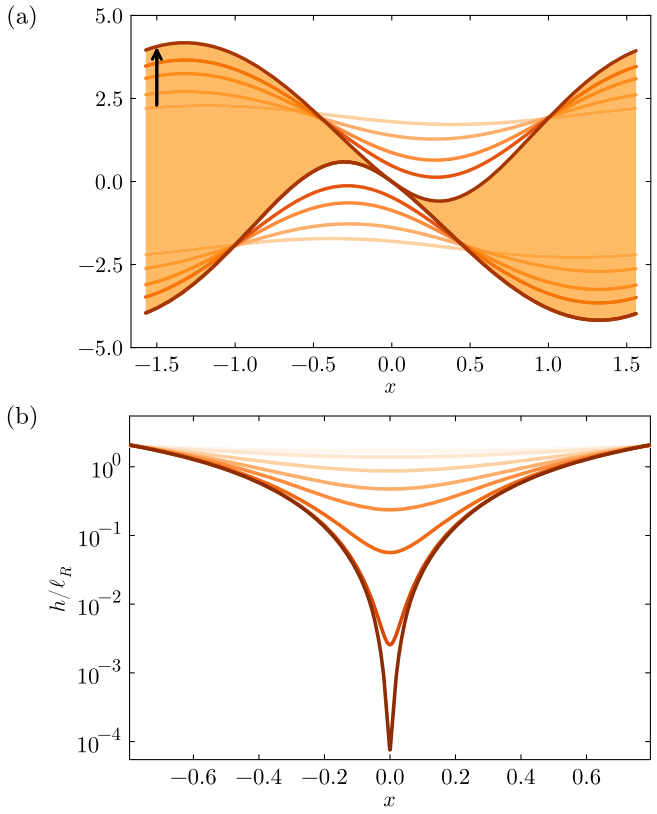


FIG. 2. (a) Numerical solution of equations (6) over a periodic domain. The light orange line shows the initial profile, and the sequence of darkening lines show the strip as time progresses; the black arrow marks the direction of time. (b) The thickness function h is symmetric about $x = 0$ as time progresses, and as breakup is approached the minimum strip thickness decreases to zero. In all plots lengths are measured in units of $\ell_R = \gamma(\eta + \eta_R)/(\eta\eta_R\Omega)$.

antisymmetric center line. The global (anti)symmetry of these shapes is a result of the initial conditions, but the symmetries were seen to hold true locally for all initial conditions we tried. The symmetry of h is demonstrated nicely in Fig. 2(b), which shows a sequence of thickness profiles as the breakup time is approached.

To check our theory against the experiment, we compare simulations run from the same, but smoothed, initial condition to the experiments shown in Fig. 1(a) with experiment. The results are shown in Fig. 3, where the experiments, shown in shades of orange, match the simulations, shown as dashed black lines. Note that in comparing the results we have used the experimental values of the parameters taken from Soni *et al.* [12] to compute ℓ_R, but adjusted the timescale. While there is not sufficient experimental data to follow the dynamics close to breakup, there is a clear transition between a linear (small deformation) and nonlinear regime.

As the moment of breakup is approached, these nonlinearities become more important and control the dynamics. To understand them, we take a closer look at Fig. 2(b) to notice that the breakup is highly localized, with the

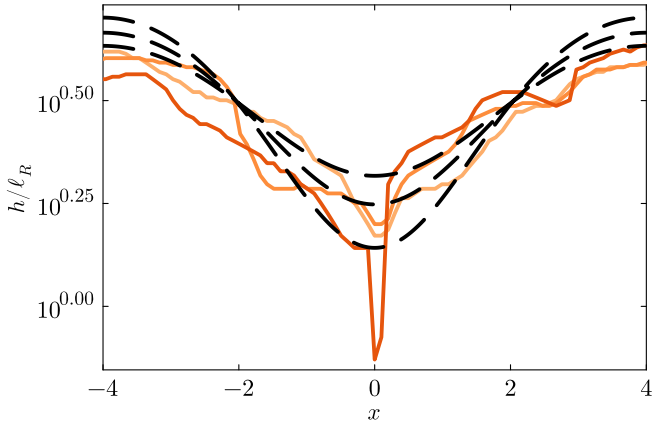


FIG. 3. Comparison between the experimental data from Fig. 1(a), shown in shades of orange, and numerical simulations, shown as dashed black lines. The simulations are initiated from an initial condition that smoothly approximated the experimental data, and each line in both sets are equally spaced in time. We see qualitative agreement between the experiment and simulation, with the timescale the only adjustable parameter.

thickness decreasing rapidly near the origin but changing slowly in the far field. This suggests that a local analysis of the pinch region will be sufficient.

Scaling theory—Because the breakup is localized, its dynamics only depends on the length and timescales that are intrinsic to Eq. (6), which are $\ell_R = \gamma(\eta + \eta_R)/(|\Omega|\eta\eta_R)$ and $t_R = \ell_R^3\Gamma/\gamma$, respectively. Measuring dimensionless distances and times to the pinch point at (x_0, t_0) with $x' = (x - x_0)/\ell_R$ and $t' = (t_0 - t)/t_R$, it is natural to assume that the system becomes self-similar as $t', x' \to 0$ [4], with

$$h(x,t) = \ell_R t'^{\alpha} f(x'/t'^{\beta}),$$
$$c_x(x,t) = -S + t'^{\alpha_2} g(x'/t'^{\beta}). \tag{7}$$

The power law prefactors show that the strip thickness decreases to zero as t'^{α}, with a universal shape given by the scaling function f. Following our simulation results we assume that the center-line slope tends to a constant value $-S$, with all spatial dependence sitting in a scaling function that rides on top [36].

As we are interested in the final stages of breakup, we substitute (7) into (6) and keep only the most dominant terms as $t' \to 0$. A dominant balance argument [4,37] reveals these to be

$$4f_\xi = g_\xi, \tag{8}$$

$$\frac{1+\alpha}{4}\xi f_\xi - \alpha f + (f f_{\xi\xi\xi})_\xi = 0, \tag{9}$$

where the similarity variable $\xi = x'/t'^{\beta}$, $\alpha_2 = \alpha$, and $\beta = (1+\alpha)/4$. Any other choice of β and α_2 is inconsistent, as other terms would become relevant as $t' \to 0$. The exponent

α remains undetermined by dominant balance, so we have self-similarity of the second kind [20]; it is later found by solving the nonlinear eigenvalue problem (9) [20].

The terms in (8) come from a balance of chirality and tension in the center-line equation; the time derivative term is negligible, and thus the center line is quasistatic in the pinch region. The thickness equation (9), comes from balancing the time derivative and the surface-tension terms in the thickness equation, and is locally equivalent to the Hele-Shaw equation when converted to similarity variables [34,38,39]. However, in the Hele-Shaw problem, a self-similar solution of the form (7) is never seen as the pinch region never becomes disconnected from the far-field [34,40,41]. In contrast, here, the linear instability set in by the chiral stress is enough to kick-start breakup and we do see self-similarity as in (7).

To find g we integrate (8), giving

$$g = 4f + g_0, \tag{10}$$

where g_0 is a constant, zero in all our simulations. The center line and thickness are hence characterized by the same scaling function f, which solves (9). This equation is fourth order with one free parameter, meaning five boundary conditions are required for a unique solution. Assuming symmetry about the pinch at $\xi = 0$ yields the first three

$$f(0) = 1, \qquad f_\xi(0) = 0, \qquad f_{\xi\xi\xi}(0) = 0, \tag{11}$$

where we have used a scale-invariance of (9) to set the value at the origin to unity. The remaining degrees of freedom are the exponent α and the second derivative at the origin $f_{\xi\xi}(0)$, which parametrize a two-dimensional space of solutions. A unique solution is picked out by enforcing the matching condition

$$f \propto \xi^{\alpha/\beta} \quad \text{as } |\xi| \to \infty, \tag{12}$$

which ensures that the thickness becomes static far from the pinch region, with t' dropping out of the scaling forms (7) as $\xi \to \infty$ [4]. As shown in Supplemental Material [33], matching corresponds to two conditions at infinity, and so (9) is now fully specified. The resulting problem is solved with the shooting method, yielding

$$\alpha \approx 1.2392, \qquad f_{\xi\xi}(0) \approx 2.7789, \tag{13}$$

as well as the solid red curve in Fig. 4(b). Comparing this scaling with results from our PDE simulations in Fig. 4(a) we see excellent agreement, with the strip thickness going to zero like $t'^{1.24}$. The scaling function found from shooting also matches simulations, with the PDE results shown as dashed lines in Fig. 4(b) collapsing onto the predicted red curve as $t' \to 0$.

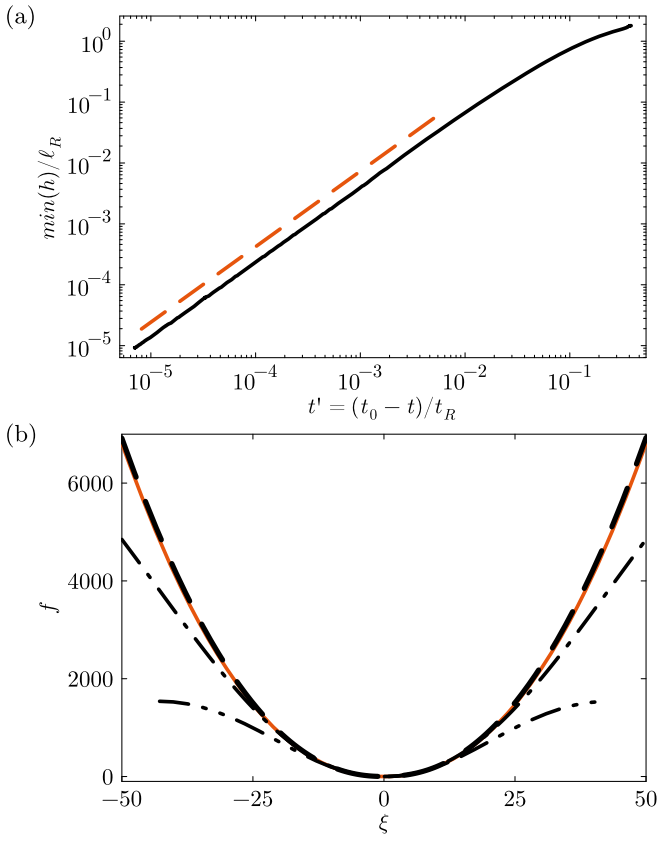


FIG. 4. (a) Scaling of the minimum strip thickness as a function of the time to breakup, t'. The black line is from the PDE simulation, and the orange dashed line is the power law $t'^{1.24}$. (b) The scaling function f. The solid orange line gives the prediction from our scaling theory; the dashed, dot-dashed, and chain-dashed lines come from the PDE simulation at $t' = 7 \times 10^{-6}, 1.8 \times 10^{-4}, 7 \times 10^{-4}$. The agreement between the PDE results and theory improves as breakup is approached.

The scaling exponent (13) could not be extracted from the experimental data as there are not enough images during the breakup process [12]. To ease measurement of scaling, it would be beneficial to increase the values of ℓ_R and t_R, which would slow and enlarge the breakup region. This could be done by using particles with a stronger magnetic moment so that the surface tension was larger [12,24].

Our scaling analysis leads to a quantitative understanding of chiral breakup, which qualitatively can be understood by the following mechanism. The initial linear instability sets the system in motion and twists the center line, resulting in a center-line-slope growing like x^k for positive k, far away from the pinch. The balance of chiral and surface tension forces in (8) means that the thickness also grows, with $h \sim x^k/4$. Substituting this into (9) we see that the power law growth causes a surface-tension drive mass current that grows like $k(k-1)(k-2)x^{2k-3}$, pumping fluid out of the pinch provided that $k > 2$. This agrees with the results from our scaling theory, as the matching condition (12) gives $k = \alpha/\beta \approx 2.2$.

To conclude, we have studied the asymmetric breakup of a strip of active chiral fluid using both asymptotic and numerical methods, showing that the breakup is driven by a combination of chiral and tension forces. As is common in fluid breakup [4], we showed that the strip took scaling form in the asymptotic regime near pinch-off, with the minimum thickness decaying to zero as a power law in finite time. Owing to novel features of the chiral dynamics, this breakup process realizes a long anticipated, but never found, similarity solution first proposed in the study of Hele-Shaw flows [34].

While breakup studies the dynamics of droplet formation, it is natural to consider the reverse problem of coalescence where two droplets merge into one [42]. This has been observed in the motivating experiments on active chiral fluids [12], but also has relevance for other active systems [7,8]. Outside of these singular problems, the asymptotic methods used here could be applied to other active matter problems where nonlinearities are relevant, such as the spreading of active films [43].

Acknowledgments—T. B. L., L. N. would like to thank the Isaac Newton Institute for Mathematical Sciences, Cambridge, for support and hospitality during the program *New statistical physics in living matter*, where part of this work was done. This work was supported by EPSRC Grants No. EP/V520287/1, No. EP/R014604/1, and No. EP/T031077/1. We thank the group of William Irvine for supplying high resolution videos of the experiments. L. N. acknowledges the support of an EPSRC studentship and thanks Henry Andralojc for many interesting discussions, and for help in understanding the symmetries of the problem.

Data availability—The data that support the findings of this article are openly available [44].

[1] J. Eggers, Nonlinear dynamics and breakup of free-surface flows, Rev. Mod. Phys. **69**, 865 (1997).
[2] J. Eggers, Universal pinching of 3D axisymmetric free-surface flow, Phys. Rev. Lett. **71**, 3458 (1993).
[3] J. Eggers and E. Villermaux, Physics of liquid jets, Rep. Prog. Phys. **71**, 036601 (2008).
[4] J. Eggers and M. A. Fontelos, *Singularities: Formation, Structure, and Propagation* (Cambridge University Press, Cambridge, England, 2015), Vol. 53.
[5] S. Ramaswamy, The mechanics and statistics of active matter, Annu. Rev. Condens. Matter Phys. **1**, 323 (2010).
[6] M. C. Marchetti, J.-F. Joanny, S. Ramaswamy, T. B. Liverpool, J. Prost, M. Rao, and R. A. Simha, Hydrodynamics of soft active matter, Rev. Mod. Phys. **85**, 1143 (2013).
[7] D. Zwicker, R. Seyboldt, C. A. Weber, A. A. Hyman, and F. Jülicher, Growth and division of active droplets provides a model for protocells, Nat. Phys. **13**, 408 (2017).
[8] R. Singh and M. E. Cates, Hydrodynamically interrupted droplet growth in scalar active matter, Phys. Rev. Lett. **123**, 148005 (2019).
[9] L. Giomi and A. DeSimone, Spontaneous division and motility in active nematic droplets, Phys. Rev. Lett. **112**, 147802 (2014).
[10] R. Adkins, I. Kolvin, Z. You, S. Witthaus, M. C. Marchetti, and Z. Dogic, Dynamics of active liquid interfaces, Science **377**, 768 (2022).
[11] E. Tjhung, C. Nardini, and M. E. Cates, Cluster phases and bubbly phase separation in active fluids: Reversal of the ostwald process, Phys. Rev. X **8**, 031080 (2018).
[12] V. Soni, E. S. Bililign, S. Magkiriadou, S. Sacanna, D. Bartolo, M. J. Shelley, and W. T. Irvine, The odd free surface flows of a colloidal chiral fluid, Nat. Phys. **15**, 1188 (2019).
[13] B. Liebchen and D. Levis, Chiral active matter, Europhys. Lett. **139**, 67001 (2022).
[14] M. Han, M. Fruchart, C. Scheibner, S. Vaikuntanathan, J. J. De Pablo, and V. Vitelli, Fluctuating hydrodynamics of chiral active fluids, Nat. Phys. **17**, 1260 (2021).
[15] C. B. Caporusso, G. Gonnella, and D. Levis, Phase coexistence and edge currents in the chiral Lennard-Jones fluid, Phys. Rev. Lett. **132**, 168201 (2024).
[16] S. Fürthauer, M. Strempel, S. W. Grill, and F. Jülicher, Active chiral fluids, Eur. Phys. J. E **35**, 1 (2012).
[17] T. Markovich and T. C. Lubensky, Odd viscosity in active matter: Microscopic origin and 3D effects, Phys. Rev. Lett. **127**, 048001 (2021).
[18] S. Ganeshan and A. G. Abanov, Odd viscosity in two-dimensional incompressible fluids, Phys. Rev. Fluids **2**, 094101 (2017).
[19] H. Massana-Cid, D. Levis, R. J. H. Hernández, I. Pagonabarraga, and P. Tierno, Arrested phase separation in chiral fluids of colloidal spinners, Phys. Rev. Res. **3**, L042021 (2021).
[20] G. I. Barenblatt, *Scaling, Self-Similarity, and Intermediate Asymptotics: Dimensional Analysis and Intermediate Asymptotics* (Cambridge University Press, Cambridge, England, 1996), p. 14.
[21] N. Goldenfeld, *Lectures on Phase Transitions and the Renormalization Group* (CRC Press, Boca Raton, 2018).
[22] L. L. Jia, W. T. Irvine, and M. J. Shelley, Incompressible active phases at an interface. Part 1. Formulation and axisymmetric odd flows, J. Fluid Mech. **951**, A36 (2022).
[23] S. Ramaswamy and G. F. Mazenko, Linear and nonlinear hydrodynamics of low-friction adsorbed systems, Phys. Rev. A **26**, 1735 (1982).
[24] A. Chaves, M. Zahn, and C. Rinaldi, Spin-up flow of ferrofluids: Asymptotic theory and experimental measurements, Phys. Fluids **20**, 053102 (2008).
[25] E. Kirkinis and M. Olvera de la Cruz, Activity-induced propulsion and separation of passive chiral particles in liquids, Phys. Rev. Fluids **8**, 023302 (2023).
[26] L. D. Landau and E. M. Lifshitz, *Fluid Mechanics: Volume 6* (Elsevier, New York, 1987), Vol. 6.
[27] Y. Zhang, J. E. Sprittles, and D. A. Lockerby, Nanoscale thin-film flows with thermal fluctuations and slip, Phys. Rev. E **102**, 053105 (2020).
[28] J. Eggers and T. F. Dupont, Drop formation in a one-dimensional approximation of the Navier–Stokes equation, J. Fluid Mech. **262**, 205 (1994).
[29] P. Howell, Models for thin viscous sheets, Eur. J. Appl. Math. **7**, 321 (1996).

[30] D. T. Papageorgiou, On the breakup of viscous liquid threads, Phys. Fluids **7**, 1529 (1995).
[31] T. Erneux and S. H. Davis, Nonlinear rupture of free films, Phys. Fluids A **5**, 1117 (1993).
[32] W. W. Zhang and J. R. Lister, Similarity solutions for van der Waals rupture of a thin film on a solid substrate, Phys. Fluids **11**, 2454 (1999).
[33] See Supplemental Material at http://link.aps.org/supplemental/10.1103/w2n2-zzkd, which presents additional details.
[34] A. L. Bertozzi, M. P. Brenner, T. F. Dupont, and L. P. Kadanoff, Singularities and similarities in interface flows, in *Trends and Perspectives in Applied Mathematics* (Springer, New York, 1994), pp. 155–208.
[35] S. A. Teukolsky, B. P. Flannery, W. Press, and W. Vetterling, Numerical recipes in c, SMRP Res. Paper **693**, 59 (1992).
[36] J. Eggers, Singularities in droplet pinching with vanishing viscosity, SIAM J. Appl. Math. **60**, 1997 (2000).
[37] C. M. Bender and S. A. Orszag, *Advanced Mathematical Methods for Scientists And Engineers I: Asymptotic Methods and Perturbation Theory* (Springer Science & Business Media, New York, 2013).
[38] J. Eggers and M. A. Fontelos, The role of self-similarity in singularities of partial differential equations, Nonlinearity **22**, R1 (2008).
[39] J. King and M. Bowen, Touchdown-singularity formation and criticality in the thin-film equation, Phil. Trans. R. Soc. A **383**, 20230375 (2025).
[40] T. F. Dupont, R. E. Goldstein, L. P. Kadanoff, and S.-M. Zhou, Finite-time singularity formation in Hele-Shaw systems, Phys. Rev. E **47**, 4182 (1993).
[41] R. Almgren, A. Bertozzi, and M. P. Brenner, Stable and unstable singularities in the unforced Hele-Shaw cell, Phys. Fluids **8**, 1356 (1996).
[42] J. Eggers, J. R. Lister, and H. A. Stone, Coalescence of liquid drops, J. Fluid Mech. **401**, 293 (1999).
[43] Y. Zhao, R. Zakine, A. Daerr, Y. Kafri, J. Tailleur, and F. van Wijland, Wetting by active fluids, Nat. Phys. **22**, 805 (2026).
[44] Luke Neville (2025), https://github.com/naturlog/chiral_break.

Correction: The source information in Ref. [43] was incorrect and has been fixed.